The Effect of Different Tropospheric Models and Ocean Tide on long Baselines.

Hamed, M.*, Shaker, A.**, Saad, A*.*, Mahmoud, S. ***

* *Faculty of Engineering, Kafer Elshekh University*
** *Shoubra faculty of Engineering ,Banha Unversity*

*** *National Recearch Institute of Astronomy and Geophysic*

Abstract:

The effect of the atmosphere has been identified as the major problem of long – baseline carrier phase positioning. The effect of the ionosphere, however, can be neutralized with dual – frequency observations. The effect of the troposphere is the challenge of precise positioning and needs to be mitigated in same way. Compensation for the tropospheric biases is often carried out using a standard tropospheric model. Most standard tropospheric models were experimentally derived using a available radiosounds data. In order to determine the best-fit standard tropospheric model with the GPS data, investigations on the impact standard tropospheric models on GPS baseline accuracy are there for needed. This paper aims to compare the GPS base lines results derived from the use of five different standard tropospheric models, and the effect of the ocean tide on the final solution . The concept behind them are presented and discussed.

Key words: - GPS observations, Tropospheric models, scientific software (Bernese)

1-Introduction

The Global Positioning System has dramatically changed the way that surveyors and other professional engineers measure positional coordinates. These experts can now measure spatial distances- base lines and estimate 3D coordinates of a new point relative to a reference located from a few to many tens of kilometers away .(**Chatzinikos, M .2006**). Static GPS is still commonly used for establishing and maintaining geodetic reference networks. It is general knowledge that accuracy of long base lines improves when precise orbits are used. Atmosphere is one of the biggest error sources in GPS measurements and it is divided into two parts: troposphere and ionosphere. The influence of the troposphere is mostly taken into account with a model and ionosphere effects are expected to vanish by using dual frequency receivers (**Jyrki, 2008)**. It is generally known that the atmospheric effects on the GPS signals are the most dominate spatially correlated biases .The atmosphere causing the delay in GPS signals consists of two main layers, ionosphere and troposphere. The ionosphere bias can be mitigated using dual frequency receivers. Unlike the ionospheric bias, the tropospheric bias cannot be removed using the same procedure. Compensation for the tropospheric bias is often carried out using a standard tropospheric model. (**Satirapad.Ch, 2004).**

2-The Troposphere

The neutral atmosphere, which is the non-ionized part of atmosphere, that stretches from the earth's surface to a height of approximately 50km, can normally be divided into two components, the hydrostatic (dry) and the wet portions of the troposphere. The hydrostatic component consists of mostly dry gases (normally referred to the dry part), whereas the wet component is a result of water vapor. The troposphere causes radio signal delay. The hydrostatic fraction contributes approximately 90% of total tropospheric refraction. (**B.Witchay ,2000)**. Tropospheric effect is frequency – independent and cannot be eliminated via dual- frequency observations. The tropospheric path delay can be broken into two components, dry and wet. The dry component

represents about 90% of the delay and can be predicted to a high degree of accuracy using mathematical models . The wet component of the tropospheric delay depends on the water vapor along the GPS signal path. Unlike the dry component, the wet component is not easy to predict.

Several mathematical models use surface meteorological measurements (atmospheric pressure, temperature and partial water vapor pressure) to compute the wet component. Unfortunately, however, the wet component is weakly correlated with surface meteorological data, which limits its prediction accuracy. It was found that using default meteorological data (1.010 mb for atmospheric pressure, 20˚ c for temperature, and 50 % for relative humidity) gives satisfactory results in most cases. (**El . Rabbany ,2002).**

The tropospheric delay can mathematically be expressed by

$$d_{Trop} = d_{zd}. m_d + d_{zwet} . m_{wet}$$

where

d_{Trop} is the total troposphere delay ,

$d_{zd,} d_{zwet}$ are the dry and wet zenith,

m_d, m_{wet} are the corresponding mapping functions which are used to map the zenith delay to the slant signal direction (**Xiangqion ,2000)**

3-Effect of Tropospheric Models on long base lines

Many models have been developed for modeling tropospheric effect, such as the Saastmoinen total delay model (**Saastamoinen ,1972,1973**), the Hopfield dual – quartic model (**Hopfield , 1969**) . In addition, different mapping functions wich illustrate signal delay as a function of elevation angle are also given (**Black ,1984**). Most of these models can very well model the dray tropspheric. This paper will discuses the effect of the tropospheric model such as (Hopfield , Saastmoinen and Niell (dry only and dry and

wet component) especially found in Bernese soft ware and select the suitable model in long base line.

3-1 Hopfield Model

The Hopfield model [**Hopfield, 1969]** is based upon a large number of meteorological radiosounds balloon profiles made at various geographical locations over a number of years . Hopfield model applies a single layer poly tropic model atmosphere ranging from the Earth surface to altitudes of about 11km and 40 km for the wet and dry layers.
Using real data covering the whole earth, has empirically found a representation of the dry refractivity as a function of the height h above the earth surface [**Hofmann ,2001]**, and is taken the following form:

$$N_d^{Trop} = N_{d,0}^{Trop} \left(\frac{H_d - h}{H_d}\right)^U$$

$$N_w^{Trop} = N_{w,0}^{Trop} \left(\frac{H_w - h}{H_w}\right)^U$$

Where $U = 4$ empirically determined power of the height ratio,
under the assumption of a poly tropic layer with thickness for dry part (m)

H_d = 40136 + 148.72 [T- 273.16]

H_w = 11000 a poly Tropic thickness for wet part (m)

3-2 Saastamoinen Model

Saastamoinen (1972-73) claims that detailed knowledge of height distribution is not necessary to determine the refractivity integral. This makes the derivation of refraction formula simpler also it improves the accuracy of this derivation. This is

because the height is directly proportional to the ground pressure in a dry atmosphere. He establishes his model on these assumptions:

1- The water vapour behaves as ideal gases,

2- The whole amount of water vapor is in the troposphere,

3- Water vapour pressure is described as **(Cetin .M, 1997)** :

$$e = e_s \left(\frac{T}{T_s}\right)^{\frac{4g^{Md}}{R_\alpha}}$$

where e_s is the surface partial water vapour pressure (mbar) , T_s is the surface temperature (K) and temperature decrease linearly with height

$$T = T_0 - \alpha\,(h - h_0)$$

3-3 Niell Mapping Function (NMF)

Niell (1996) kept the basic form of the Herring (MTT model , Herring 1992) mapping function adding a height correction term and assuming that the elevation dependence is a function of only geographical parameters and developed expressions for calculating the mapping function for both the hydrostatic and wet delay for elevation angle down to 3 degrees. He used three terms of the Marini continued fraction form. His model takes the same shape as Herring, but, his parameters a, b and c for the hydrostatic mapping function are formulated as a function of latitude, height above sea level of the observing site and the day of year (if we accept that in a way the day of the year is also a constant and independent parameter) and proposed the function (**Pikrida,C. (2006**).

$$\mathrm{m(E)} = \frac{1 + \dfrac{a}{1 + \dfrac{b}{1 + c}}}{\sin(\mathrm{E}) + \dfrac{\mathrm{a}}{\sin(\mathrm{E}) + c}} + \Delta m(E)$$

4- Used data

The test area cantinas five points as following PHLW in Helwan , SFAG in Sfaga, SHLA in Shlatin , SLUM in Slum and ALIS in Aswan , and a selected GPS permanent stations (IGS) distributed in a second test area which represent long baselines namely, BAHR in (Bahrain) , RAMO in (Israel) and NICO in(Cyprus) fig (1) . The coordinates of the (IGS)control points were estimated in ITRF2000 at the day of the observing campaign (5 Dec.. 2007), GPS week (1456) and site velocities given by the IERS (http : // itrf. ensg. ign fr) by using the formula**:[Altamimi . Z,2006]**

$$P(t) = P(t_0) + \dot{P}(t-t_0)$$

Where:

t_0 is value at a reference epoch

t its value at time t

$\dot{P}$ is the velocity

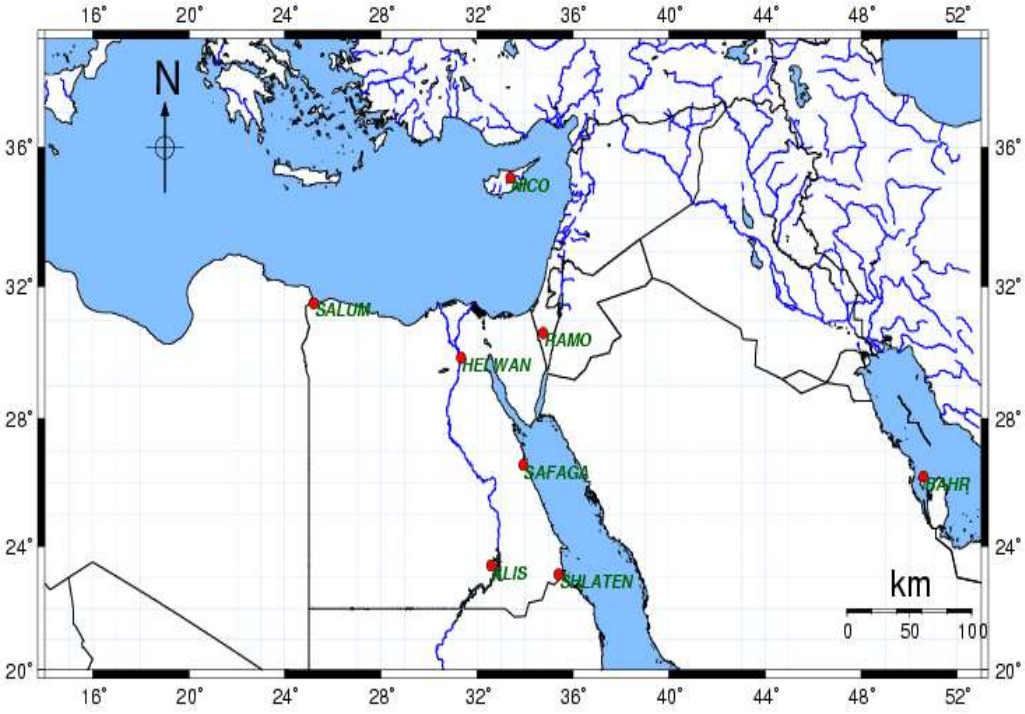

Fig. (1) :data used

4-1 Data Analysis

Ten lines were selected to represent the long base lines table(1). The GPSEST which is programmed in Bernese software is used to test all available models delay for the present data. The tropospheric delay models used here are Hopfield , Saastamoinen , Niell, Dry Hopfield , Dry Saastamoinen, Dry Niell and the case of none model .
Different elevation angles (3,5,10,15,20,50) are used in analysis in every model and the mean is taken for all cases and the optimum model is selected.

Table (1) :- represent baselines used in processing

Baseline Name	Abbreviations	Baseline length
Alis-Shalatin	ALSH	288901.2923
Alis-Bahr	ALBA	1840081.4057
Shlatine-Bhar	SHBA	1572321.6165
Shlatine-Ramo	SHRA	831869.4773
Ramo-Safga	RASA	453989.4846
Slume-Ramo	SLRA	916085.6805
Nico-Slume	NISL	861855.3591
Bahr-Nico	BANI	1912201.2296
Nico-Ramo	NIRA	519734.3187
Shlatin-Slum	SHSL	1367214.1244

Table (2) :- represent mean RMS (m) in all models and represent the optimum model

	HOP	SAAST	NIELL	DHOP	DSAAST	DNELL	NON
BASELINE	RMS	RMS	RMS	RMS	RMS	RMS	RMS
ALSH	0.0044	0.0045	0.0046	0.0064	0.0067	0.0072	0.0644
ALBA	0.0047	0.0048	0.0049	0.0068	0.0071	0.0072	0.0666
SHBA	0.0046	0.0048	0.0049	0.0067	0.0070	0.0071	0.0650
SHRA	0.0038	0.0040	0.0041	0.0058	0.0060	0.0061	0.0498
RASA	0.0041	0.0043	0.0044	0.0061	0.0065	0.0065	0.0556
SLRA	0.0038	0.0040	0.0041	0.0057	0.0060	0.0061	0.0538
NISL	0.0042	0.0044	0.0045	0.0062	0.0065	0.0066	0.0592
BANI	0.0018	0.0019	0.0020	0.0028	0.0029	0.0029	0.0258
NIRA	0.0038	0.0040	0.0041	0.0057	0.0060	0.0061	0.0507
SHSL	0.0040	0.0042	0.0043	0.0061	0.0064	0.0064	0.0583
Mean	**0.0039**	**0.0041**	**0.0042**	**0.0058**	**0.0061**	**0.0062**	**0.0549**

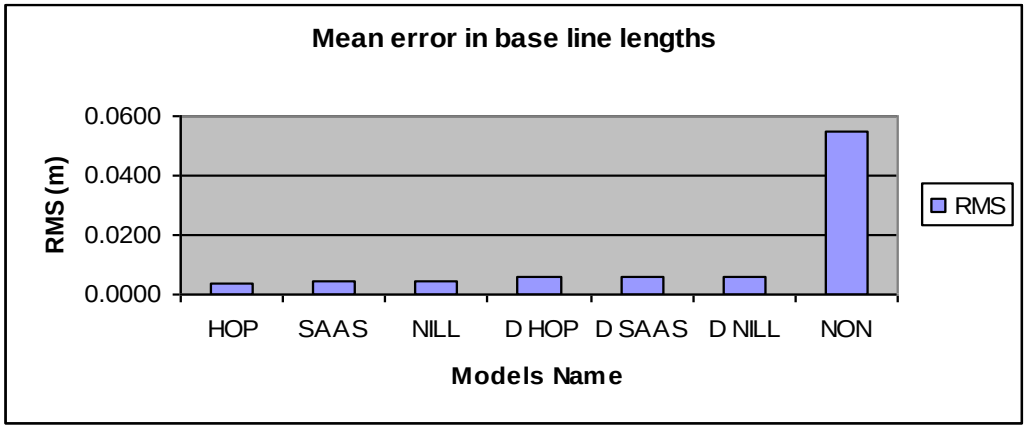

Fig. (2): Error in baseline length (mm)

Table (3) :The displacement in baseline lengths related to optimum model (Hopfield) in (ppm)

NO.	Baselines	Optimum lengths in Hop	Hop-Saast	Hop-Niell	Hop-Dhop	Hop-Dsaast	Hop-Dniell	Hop-Non
1	ALSH	288901.2930	0.0048	0.0060	0.0239	0.0377	0.0286	0.8628
2	ALBA	1840081.3968	0.0038	0.0048	0.0330	0.0406	0.0350	0.8166
3	SHBA	1572321.6048	0.0038	0.0050	0.0357	0.0425	0.0377	0.8135
4	SHRA	831869.4745	0.0023	0.0033	0.0284	0.0314	0.0321	0.8628
5	RASA	453989.4818	0.0022	0.0035	0.0275	0.0288	0.0297	0.7673
6	SLRA	916085.6806	0.0090	0.0102	0.0349	0.0385	0.0382	0.9277
7	NISL	861855.3585	0.0013	0.0024	0.0395	0.0407	0.0439	0.9710
8	BANI	1912201.2131	0.0027	0.0036	0.0371	0.0420	0.0401	0.8231
9	NIRA	519734.3184	0.0055	0.0063	0.0280	0.0311	0.0312	0.9408
10	SHSL	1367214.1186	0.0018	0.0029	0.0405	0.0434	0.0458	0.9106

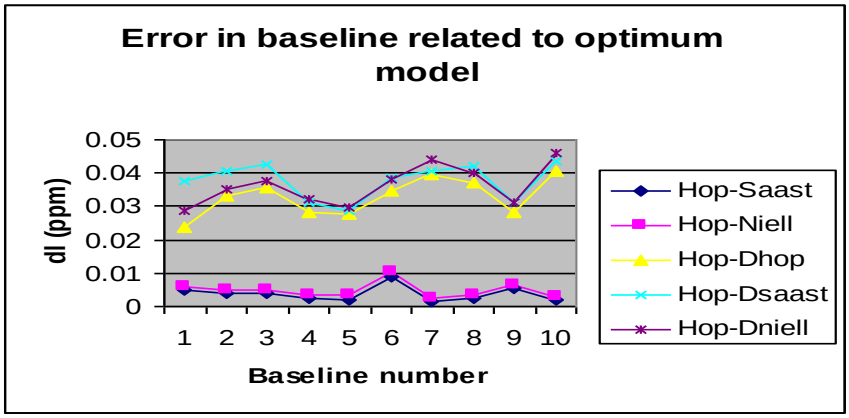

Fig. (3). Error in baseline lengths (ppm) related to optimum model

Table (4) :- represent mean RMS in baseline heights in all models

NO.	BASELINE	HOP RMS	SAAST RMS	NIELL RMS	DHOP RMS	DSAAST RMS	DNELL RMS	NON RMS
1	ALSH	0.0054	0.0055	0.0056	0.0076	0.0079	0.0080	0.0655
2	ALBA	0.0057	0.0058	0.0059	0.0079	0.0083	0.0084	0.0674
3	SHBA	0.0056	0.0056	0.0057	0.0077	0.0081	0.0082	0.0662
4	SHRA	0.0050	0.0052	0.0053	0.0073	0.0076	0.0077	0.0627
5	RASA	0.0052	0.0053	0.0054	0.0074	0.0078	0.0078	0.0669
6	SLRA	0.0043	0.0045	0.0046	0.0064	0.0067	0.0067	0.0541
7	NISL	0.0043	0.0045	0.0046	0.0064	0.0067	0.0067	0.0541
8	BANI	0.0055	0.0056	0.0057	0.0077	0.0080	0.0081	0.0650
9	NIRA	0.0044	0.0046	0.0047	0.0064	0.0068	0.0068	0.0546
10	SHSL	0.0050	0.0052	0.0053	0.0073	0.0076	0.0077	0.0627

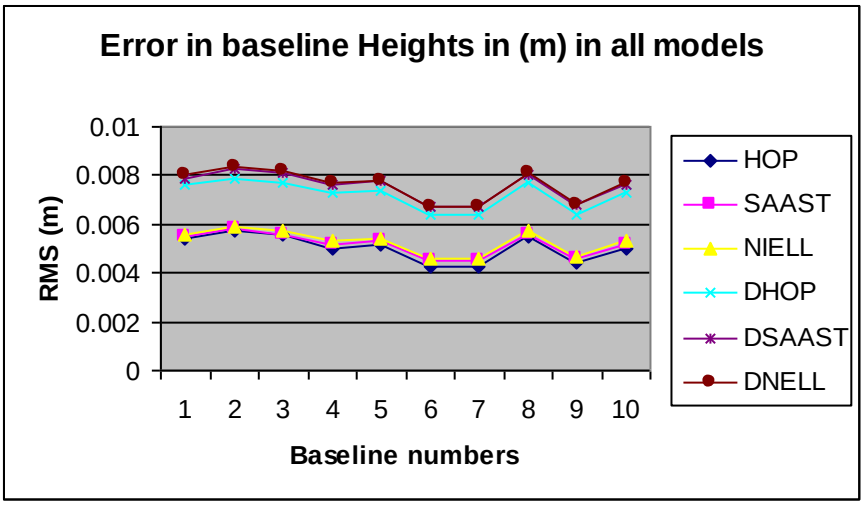

Fig.(4). Error in baseline Heights in (m)

5- Ocean Tide

Tides can be defined as periodic movements which are directly related in amplitude and phase to some periodic geophysical force. The dominate geophysical force, which cause gravitational attraction of moon and sun on the surface of the earth (**Mazhar.R and Marcelo .S ,2004**)

5-1 Ocean tide loading (OTL)

Earth body tides refer to as the elastic deformation of the earth due to tidal forces of the sun , moon and planets, causing time- dependent variation in station heights. The elastic deformation of the Earth's crust due to ocean tide loading produces a site displacement in the order of a few centimeters for the vertical component and less than one third for the horizontal components. On the other hand, the increasing precision of space geodetic measurements has provided a new interest for the evaluation of these load effects, since they have to be applied in the analysis of most space geodetic observations if highest accuracy has to be achieved. The ocean loading values for each station can be acquired via Internet on ~loading.http://www.oso.chalmers.se/the Onsala site.
Apriori file is needed here from the Bernese computation which carries the approximate geocentric values, if a best final geocentric values of each station is required. These geocentric values of each station are forwarded to the Onsala site before the ocean loading files can be computed and used as the ocean loading correction files in the Bernese processing.

5-2 Results

We notice that, influence in the (X,Y,Z) axis after and before apply the OTL, between (o.1-3.5mm),(0.2 -5.7mm), (0.1-2.6mm) respectively ,and influence at the height increases ranging between (0.2-6.7mm) especially at points such as (BAHR, ,PHLW) fig (5)

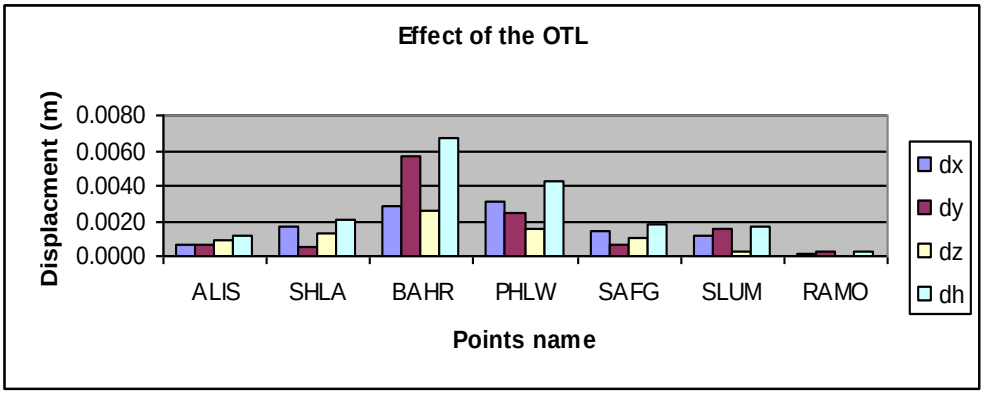

Fig (5): represent effect of the OTL at points

6- Conclusions

We notice that. When taking the mean for the RMS in base lines at different elevation angles and different models table (8) , the RMS values in baselines in case of Hopfield model are small for all different angles compared to other models fig (2), so Hopfield model is the optimum model on long base lines. The displacement in base line between the optimum model and another model refer to the optimum model different from Saastamoinen by value ranging from (0.0013 to 0.0055ppm) , Niell by (0.0033 to 0.01ppm) , dry Hopfield by (0.023 to 0.041ppm) ,dry Saastamoinen by (0.028 to 0.042ppm) and dry Niell by (0.028 to 0.045 ppm), so, Saastamoinen model is closest to the Hopfield and then followed by Niell but the dry part such as (dry hop., dry saast, dry niell) differ by large values (0.94 ppm) ,so that , the dry part is a poor choice. And also for the effect OTL we notice that, the displacement in heights increases in the range of (0.2 – 6.7m m) .So you can not ignore this effect , especially points of low height and the points near any beach.

7- Recommendations

In long baselines and precise work and according to the results obtained it is recommended to

1- Use Hopfield model as it gives satisfactory results over the other models.

2-We can not neglect the impact of the OTL correction because it affects the accuracy of the solution.

References

Altamimi. Z.(2006). "IGS reference frames : Status and future improvements , Institute Geographique National , France.

Boonsap Witchayangkoon. (2000)." Elements of GPS precise point positioning , ph.D, University of Technology Thonburi, Bangkok.

Black H.D.(1984)." Correcting satellite Doppler data for tropospheric effects . Journal of Geophysical Research, Vol. 89, No. D4, pp. 2616-2626.

Chatzinikos .M. (2006)." Long Distance GPS Baseline Solutions Using Various Software and EPN, Greece.

Cetin. M .(1997) ." Tropospheric delay models in GPS , Istanbul / Turkey, September

15-18, 1997

EL-Rabany, A., (2002)." The Global Positioning System , Univerity of New Brunswick , Canda.

Herring ,T.A. (1992) . "Modelling Atmospheric Delay in the Analysis of Space Geodetic Data, Symposium of Transatmospheric Signals in Geodesy, Netherlans Geod. Commis. Ser.36,1992,pp.157-164, Ned.Comm. Voor Geod.,Delft.

Hofmann- Wellenhof ,B. (2001)." Global positioning system. Theory and practice, Fifth revised edition, Spinger-Verlag, New York

Hopfield , H.S. (1969). " Two – quartic tropospheric refractivity profile for correcting satellite data ", Journal of Geophysical Research , 74,4487-4499

Hopfield , H.S. (1971)." Tropospheric Effect on Electromagnetic cally Measured Range : Prediction from Surface WeatherData ", Radio Science , vol. 6, pp.357-36

Jyrki Puupponen, Pasi Häkli and Hannu Koivula. (2008)."Influence of Global Ionosphere Model in Static GPS Surveying using Commercial GPS Processing Software. Stockholm, Sweden.

Niell, A.E.(1996). " Global Mapping Function for the Atmospheric Delay at Radio Wavelengths. Journal of Geophsical Research, Vo1.101,No.B2 pp.3227-3246

Pikridas ,C. , Rossikopoulos , D. , Katsougiannopoulos , S.(2006). " Tropospheric refraction estimation using various models radiosonde measurement and permanent GPS data. University of Greece , Germany

Saastamoinen, J. (1972)." Atmospheric Correction for the Troposphere and Stratosphere in Radio Ranging of Satellites "Monogr. Ser., vol.15,pp.247-251.

Saastamoinen, J. (1973)."Contribution to the theory of atmospheric refraction "Bulletin Geodesique, 107,13-34.

Satirapod, Ch .(2004)," Impact of Different Tropospheric Models on GPS Baseline Accuracy : Case study in Thailand.

Rafiq.M and Santos .(2004)," Study Eastern Canadian site displacement due to ocean tide loading using a GPS network in Atlantic Canada , University of new Brunswick Department of Geodesy and Geomtic Engineering Fredericton ,N,B ., E3B5A3, Canda.

Xiangqion, L. (2000). " Carrier phase Based Ionosphere Recovery Over A Regional Area GPS Network, University of Calgary